Universität des Saarlandes

Fachrichtung 6.1 – Mathematik

Preprint Nr. 161

Mathematical Morphology for Tensor Data Induced by the Loewner Ordering in Higher Dimensions

Bernhard Burgeth, Nils Papenberg, Andres Bruhn,
Martin Welk and Joachim Weickert

Saarbrücken 2005

Fachrichtung 6.1 – Mathematik
Universität des Saarlandes

Preprint No. 161
submitted: December 14, 2005

Mathematical Morphology for Tensor Data Induced by the Loewner Ordering in Higher Dimensions

Bernhard Burgeth
Mathematical Image Analysis Group
Faculty of Mathematics and Computer Science
Saarland University, Building E 2 4
66041 Saarbrücken, Germany
burgeth@mia.uni-saarland.de

Nils Papenberg
Faculty of Mathematics
University of Lübeck
Wallstrasse 40
23560 Lübeck, Germany
papenber@math.uni-luebeck.de

Andres Bruhn
Mathematical Image Analysis Group
Faculty of Mathematics and Computer Science
Saarland University, Building E 2 4
66041 Saarbrücken, Germany
bruhn@mia.uni-saarland.de

Martin Welk
Mathematical Image Analysis Group
Faculty of Mathematics and Computer Science
Saarland University, Building E 2 4
66041 Saarbrücken, Germany
welk@mia.uni-saarland.de

Joachim Weickert
Mathematical Image Analysis Group
Faculty of Mathematics and Computer Science
Saarland University, Building E 2 4
66041 Saarbrücken, Germany
weickert@mia.uni-saarland.de

Edited by
FR 6.1 – Mathematik
Universität des Saarlandes
Postfach 15 11 50
66041 Saarbrücken
Germany

Fax: + 49 681 302 4443
e-Mail: preprint@math.uni-sb.de
WWW: http://www.math.uni-sb.de/

Abstract

Positive semidefinite matrix fields are becoming increasingly important in digital imaging. One reason for this tendency consists of the introduction of diffusion tensor magnetic resonance imaging (DT-MRI). In order to perform shape analysis, enhancement or segmentation of such tensor fields, appropriate image processing tools must be developed. This paper extends fundamental morphological operations to the matrix-valued setting. We start by presenting novel definitions for the maximum and minimum of a set of matrices since these notions lie at the heart of the morphological operations. In contrast to naive approaches like the component-wise maximum or minimum of the matrix channels, our approach is based on the Loewner ordering for symmetric matrices. The notions of maximum and minimum deduced from this partial ordering satisfy desirable properties such as rotation invariance, preservation of positive semidefiniteness, and continuous dependence on the input data. We introduce erosion, dilation, opening, closing, top hats, morphological derivatives, shock filters, and mid-range filters for positive semidefinite matrix-valued images. These morphological operations incorporate information simultaneously from all matrix channels rather than treating them independently. Experiments on DT-MRI images with ball- and rod-shaped structuring elements illustrate the properties and performance of our morphological operators for matrix-valued data.

Key Words: mathematical morphology, Loewner ordering, dilation, erosion, opening, closing, top hats, morphological derivatives, shock filter, mid-range filter, matrix-valued imaging, DT-MRI.

1 Introduction

1.1 Motivation and State-of-the-Art

For four decades, mathematical morphology has been able to respond adequately to the needs of the image processing community: Starting with Matheron's and Serra's pioneering work on binary morphology in the sixties [39, 51], generalisations to greyscale morphology have been developed in the eighties [29, 55]. Further progress has been achieved by proposals on how to extend these concepts to vector-valued images [16, 37, 57] and image sequences [22]. In the meantime morphological operators and filters are used for noise suppression, edge detection, shape analysis, image enhancement and segmentation in a number of application fields ranging from medical imaging to geological sciences. The numerous aspects of mathematical morphology

are well documented in a number of monographs [32, 40, 52, 53, 54] and conference proceedings [23, 33, 56]. However, one aspect of current image processing that has not yet received sufficient attention by the morphological community is the processing of *tensor-valued* images with morphological methods. This is the goal of the present paper. Tensor fields gained significant importance for at least three reasons:

- First, *diffusion tensor magnetic resonance imaging (DT-MRI)* [6] constitutes a modern medical imaging technique that measures a 3×3 positive semidefinite matrix-field: A so-called diffusion tensor is assigned to each voxel. This diffusion tensor describes the diffusive property of water molecules and as such is intimately related to the geometry and organisation of the tissue being examined. Water diffuses preferably along ordered tissue. Hence the matrix field is a valuable source of information for the diagnosis of multiple sclerosis and strokes [45].

- Second, tensor concepts have turned out to be very fruitful in image analysis itself [24]: The *structure tensor* [19], for instance, (also called Förstner interest operator, second moment matrix or scatter matrix) is used for motion [8] and texture analysis [47], but also for corner detection [31]. Another example is *tensor voting* [41], which is an interesting recent tool for segmentation and grouping.

- Third, in solid mechanics and civil engineering inertia, diffusion and permittivity tensors and stress-strain relationships are important tools to describe anisotropic behaviour in general.

The variety of applications requires the development of appropriate tools for the processing and analysis of matrix-valued data. Just as in the scalar case one has to remove noise, enhance structures and to detect edges and shapes by appropriate filters.
The processing of matrix-valued images is a recent area of research. The simplest strategy consists of treating all channels independently. For DT-MRI, this has been done both for shift-invariant linear filters [63] as well as for adaptive nonlinear filters [27]. Such strategies have the drawback of ignoring any relation between the different matrix channels. More advanced techniques have been proposed where derived joint expressions such as the eigenvalues and eigenvectors of the tensor field [17, 46, 58] or its fractional anisotropy [44] are smoothed. This comes down to scalar- or vector-valued filtering again.
Matrix-valued image processing methods that truly exploit the interaction of the different matrix channels have been introduced for nonlinear regularisation methods and related diffusion filters [58, 61]. The resulting nonlinear

structure tensor [61] has shown its use in motion estimation [11], texture analysis [49] and unsupervised segmentation [10]. Level set ideas in terms of mean curvature motion, self-snakes and geodesic active contour models have been generalised to the matrix-valued setting in [18], and it was also possible to design median filters [62] and homomorphic filters [15] for tensor fields.
In the present paper we will introduce a framework for tensor-valued morphological operations such as dilation, erosion and a number of filters that are based on them. Let us first discuss why this is a nontrivial task.

1.2 Difficulties

The concepts of scalar-valued morphology cannot be transferred directly even to the vector-valued cases such as colour images: Component-wise performance of standard morphological operations might result in the corruption of information in the image, since the components in general exhibit a strong correlation [2, 22].
All of the numerous attempts to develop satisfactory morphological operators for colour images, as well as for other vector-valued data, have to struggle with the difficulty that morphology is based on the notion of minimum and maximum. Hence it seems to be essential to establish an ordering of colours or vectors, but a generally accepted definition of such an ordering is not available. Different types of orderings such as marginal or reduced ordering [3] are reported to result in an unacceptable alteration of colour balance and object boundaries in the image [16], or in the existence of more than one maximum (minimum) creating ambiguities in the output image [37]. Relations between inf-sup operations, median filters and geometric partial differential equations [25] were extended from the scalar to the vectorial case in [14], while morphological filters relying on vector ranking concepts [3] have been proposed in [30, 16] for noise suppression. Clearly, the development of morphological operators for vector-valued images is decisively hindered by the lack of appropriate orderings on vector spaces.
Interestingly, the situation in the matrix-valued setting is more promising on a second glance since matrices have a richer analytic-algebraic or geometric structure in comparison to vectors:

(a) One can multiply matrices, define polynomials and can even apply functions to matrices by means of their eigenvalue decomposition.

(b) Real symmetric, positive definite matrices can be graphically represented by ellipses (2×2-matrices) or ellipsoids (3×3-matrices).

However, the morphological operations to be defined have to satisfy additional conditions such as:

(i) Rotational invariance.

(ii) Preservation of the positive semidefinitenss of the matrix field since DT-MRI data sets, for instance, posses this property.

(iii) Continuous dependence of the basic morphological operations on the matrices used as input. This is of utmost importance for the definition of morphological gradients for matrix fields.

Remarkably, the requirement of rotational invariance already rules out a straightforward componentwise approach as it is shown already in [12].

1.3 Our Contributions

In this paper we will introduce a novel notion of the maximum/minimum of a finite set of positive semidefinite matrices. This notion will exhibit the above mentioned properties of rotational invariance, preservation of positive semidefiniteness and continuity. In defining it we will be guided by the algebraic and geometric properties of the matrices under consideration. The concepts of minimum and maximum of matrices put us in the position to generalise a number of fundamental morphological operations to the tensor-valued setting. These matrix-valued morphological operations are then validated by applying them to DT-MRI images.
Two suggestions have been made on how to extend classical morphological operations such as dilation, erosion, opening and closing to matrix-valued data sets in [12]. However, lacking continuity properties of these approaches forestalled the development of morphological derivatives for matrix fields. In order to overcome this inadequacy a novel approach based on the so-called Loewner ordering for 2×2 matrices has been proposed in [13]. However, the technique used in [13] cannot be extended directly to higher-order matrices. In the present paper we use tools from convex analysis to investigate the Loewner ordering for symmetric $n \times n$-matrices with $n \geq 3$ and its usage to determine morphological operators.
The article is structured as follows: The next section is devoted to a brief review of the grey scale morphological operations we aim to extend to the matrix-valued setting: dilation, erosion, opening, closing, top hats, morphological derivatives, shock filter, and mid-range filter. In Section 3 we introduce the crucial max- and min-operations for matrix-valued data that satisfy a number of useful properties. In Section 4 these notions are used for generalising classical morphological operations to the tensor-valued setting. We report on the results of our experiments with various morphological op-

erators applied to real-world DT-MRI data in Section 5. In Section 6 we conclude the paper with a summary.

2 Scalar-Valued Morphology

In this section we briefly review the definitions of some fundamental scalar-valued morphological operators that we will generalise to the tensor-valued setting.
In grey scale morphology an image is represented by a scalar function $f(x, y)$ with $(x, y) \in \mathbb{R}^2$. The so-called *structuring element* is a set $B \subset \mathbb{R}^2$ that determines the neighbourhood relation of pixels with respect to a shape analysis task. Often convex sets such as disks, ellipses or squares are used as structuring elements.
Grey scale *dilation* $\oplus$ replaces the greyvalue of the image $f(x, y)$ by its supremum/maximum within a mask defined by B:

$$(f \oplus B)(x, y) \;:=\; \sup\{f(x-x',\, y-y') \mid (x', y') \in B\},$$

while *erosion* $\ominus$ is determined by taking the infimum/minimum:

$$(f \ominus B)(x, y) \;:=\; \inf\{f(x+x',\, y+y') \mid (x', y') \in B\}.$$

The *opening* operation, denoted by $\circ$, is defined as erosion followed by dilation:

$$f \circ B := (f \ominus B) \oplus B\,.$$

Closing, indicated by the symbol $\bullet$, consists of a dilation followed by an erosion:

$$f \bullet B := (f \oplus B) \ominus B\,.$$

These operations form the basis of many other processes in mathematical morphology [52, 54] such as the *white top-hat* which is the difference between the original image and its opening:

$$\mathrm{WTH}(f) := f - (f \circ B)\,.$$

Its dual, the *black top-hat* is the difference between the closing and the original image,

$$\mathrm{BTH}(f) := (f \bullet B) - f\,,$$

while the *self-dual top-hat* is the difference between closing and opening:

$$\mathrm{SDTH}(f) := (f \bullet B) - (f \circ B)\,.$$

In an image the boundaries or edges of objects are the loci of high grey value variations. These variations can be detected by derivative operators such as the gradient or the Laplacian. Erosion and dilation are also the elementary building blocks of the basic morphological gradients: The so-called *Beucher gradient* [7] is the difference between the dilation and the erosion:

$$\varrho_B f := (f \oplus B) - (f \ominus B)\,.$$

It is an analog to the Euclidean norm of the gradient $|\nabla f|$ if an image is regarded as a differentiable function. More precisely, for a differentiable image f and disk-shaped structuring element B_h of radius $h > 0$ the expression

$$\frac{\varrho_{B_h} f}{2h} = \frac{(f \oplus B_h) - (f \ominus B_h)}{2h}$$

tends to $|\nabla f|$ if h goes to zero. Observe that $|\nabla f|$ equals the directional derivative $\partial_\eta f$ where $\eta := \nabla f / |\nabla f|$ gives the direction of the steepest ascent. This can also be expressed as $\sup_{\nu \in S^2} \partial_\nu f$. Here S^2 denotes the unit circle in $\mathbb{R}^3$.

We also consider the *internal gradient* as the difference between the original image and its erosion,

$$\varrho_B^- f := f - (f \ominus B)\,,$$

and the *external gradient* as the difference between the dilation and the original image:

$$\varrho_B^+ f := (f \oplus B) - f\,.$$

In the differentiable case both one-sided gradients also approximate $|\nabla f|$.

It is also possible to define morphological analogs to the Laplacian $\Delta f = \nabla^\top (\nabla f)$. The *morphological Laplacian* [59] we consider is given by the difference between external and internal gradient:

$$\Delta_B f := \varrho_B^+ f - \varrho_B^- f = (f \oplus B) - 2 \cdot f + (f \ominus B)\,.$$

This operator is not exactly a Laplacian: It approximates the second directional derivative $\partial_{\eta\eta} f$ where η denotes again the direction of the steepest slope. It allows us to distinguish between influence zones of minima and maxima: Regions with $\Delta_B f < 0$ are regarded as influence zones of maxima, while regions with $\Delta_B f > 0$ are influence zones of minima. The zero-crossings $\Delta_B f = 0$ can be interpreted as edge locations [38, 28, 35].

Morphological Laplacians are useful for designing so-called *shock filters* [36, 43, 26]. The idea behind this morphological image enhancement method is

to apply dilations around maxima and erosions around minima:

$$S_B f := \begin{cases} f \oplus B & (\Delta_B f < 0), \\ f & (\Delta_B f = 0), \\ f \ominus B & (\Delta_B f > 0). \end{cases}$$

Many variants of shock filters can be found in the literature [1, 21, 42, 48, 50, 60]. When they are applied iteratively, experiments show that their steady state is given by a piecewise constant segmentation with discontinuities ("shocks") between adjacent segments.
Although not always considered as an morphological filter we include the mid-range filter in our selection of operators:

$$\mathrm{mid}_B f := \frac{1}{2}\big((f \oplus B) + (f \ominus B)\big)\,.$$

3 Supremum and Infimum of a Set of Matrices

All morphological operations in the previous section result from suitable combinations of dilations and erosions, i.e. they come down to maximum and minimum operations. Thus, a suitable notion of maximum and minimum of a set of symmetric matrices is the key to the definition of morphological operations for tensor images. We start with a very brief account of some notions from convex analysis necessary for the following.

3.1 Notions from Convex Analysis

A subset C of a vector space V is named *cone*, if it is stable under addition and multiplication with a positive scalar. A subset B of a cone C is called *base* if every $y \in C, y \neq 0$ admits a unique representation as $y = r \cdot x$ with $x \in B$ and $r > 0$. We will only consider a cone with a convex and compact base.
The most important points of a closed convex set are its *extreme points* characterised as follows: A point x is an extreme point of a convex compact subset $S \subset V$ of a vector space V if and only if $S \setminus \{x\}$ is still convex. The set of all extreme points of S is denoted $\mathrm{ext}(S)$. All extreme points are necessarily boundary points, $\mathrm{ext}(S) \subset \mathrm{bd}(S)$. According to the theorems of Minkowski or Krein-Milman each convex compact set S in a space of finite dimension can be reconstructed as the set of all convex combinations of its extreme points [4, 34]:

$$S = \mathrm{convexhull}(\mathrm{ext}(S)).$$

We will explore these notions in connection with $\mathrm{Sym}(n)$, the vector space of symmetric $n \times n$-matrices with real entries.

3.2 The Cone of the Loewner Ordering

$\mathrm{Sym}(n)$ is endowed with the scalar product $\langle A, B\rangle := \sqrt{\mathrm{trace}(A^\top B)}$. The corresponding norm is the Frobenius norm for matrices: $\|A\| = \sum_{i,j=1}^{n} a_{ij}$.
There is also a natural partial ordering on $\mathrm{Sym}(n)$, the so-called *Loewner ordering* defined via the cone of positive semidefinite matrices $\mathrm{Sym}^+(n)$ by

$$A, B \in \mathrm{Sym}(n): \quad A \geq B :\Leftrightarrow A - B \in \mathrm{Sym}^+(n),$$

i.e. if and only if $A - B$ is positive semidefinite.
Note that this partial ordering is *not* a lattice ordering, that is to say, the notion of a unique supremum and infimum with respect to this ordering does not exist [9].
The (topological) interior of $\mathrm{Sym}^+(n)$ is the cone of positive definite matrices, while its boundary $\mathrm{bd}(\mathrm{Sym}(n))$ consists of all matrices in $\mathrm{Sym}(n)$ with a rank strictly smaller than n. It is easy to see that, for example, the set $\{M \in \mathrm{Sym}^+(n) : \mathrm{trace}(M) = 1\}$ is a convex and compact base of the cone $\mathrm{Sym}^+(\mathrm{n})$. Furthermore, it is known [4] that the matrices $v\,v^\top$ with unit vectors $v \in \mathbb{R}^n$, $\|v\| = 1$, are the extreme points of the set $\{M \in \mathrm{Sym}^+(n) : \mathrm{trace}(M) = 1\}$ [4]. They have by construction rank 1 and for any unit vector v we find $v\,v^\top v = v \cdot \|v\|^2 = v$ which implies that 1 is the only non-zero eigenvalue. Hence $\mathrm{trace}(v\,v^\top) = 1$. Because of this extremal property the set of matrices $v\,v^\top$ with $\|v\| = 1$ carries the complete information about the base of Loewner ordering cone:
convexhull($\{v\,v^\top : v \in \mathbb{R}^n, \|v\| = 1\}$) is a base for the Loewner ordering cone.
The *penumbra* $P(M)$ of a matrix $M \in \mathrm{Sym}(n)$ is the set of matrices N that are smaller than M w.r.t. the Loewner ordering:

$$P(M) := \{N \in \mathrm{Sym}(n) : N \leq M\} = M - \mathrm{Sym}^+(n)\,,$$

where we used the customary notation $a + r\,S := \{a + r \cdot s : s \in S\}$ for a point $a \in V$, a scalar r and a subset $S \subset V$. Using this geometric description the problem of finding the maximum of a set of matrices $\{A_1, \ldots, A_m\}$ amounts to determining the minimal penumbra covering their penumbras $P(A_1), \ldots, P(A_m)$. Its vertex represents the wanted maximal matrix $\overline{A}$ that dominates all A_i w.r.t the Loewner ordering. However,

the cone itself is too complicated a structure to be handled directly. Instead we associate with each matrix $M \in \mathrm{Sym}(n)$ a *ball* in the subspace $\{A : \mathrm{trace}(A) = 0\}$ of all matrices with zero trace as a *completely descriptive set*. We will assume for the sake of simplicity that $\mathrm{trace}(M) \geq 0$. This ball is constructed in two steps: First, from the statements above we infer that the set $\big\{M - \mathrm{trace}(M) \cdot \mathrm{convexhull}\{v\, v^\top : v \in \mathbb{R}, \|v\| = 1\}\big\}$ is a base for $P(M)$ contained in the subspace $\{A : \mathrm{trace}(A) = 0\}$. We observe that the identity matrix E is perpendicular to the matrices A from this subspace, $\langle A, E\rangle = \sqrt{\mathrm{trace}(A)} = 0$, and hence the orthogonal projection of M onto $\{A : \mathrm{trace}(A) = 0\}$ is given by

$$m := M - \frac{\mathrm{trace}(M)}{n} E\,. \tag{1}$$

Second, the extreme points of the base of $P(M)$ are lying on a sphere with center m and radius

$$r := \|M - \mathrm{trace}(M) v\, v^\top - m\| = \mathrm{trace}(M)\sqrt{1 - \frac{1}{n}}\,. \tag{2}$$

Consequently, if the center m and radius r of a sphere in $\{A \in \mathrm{Sym}(n) : \mathrm{trace}(A) = 0\}$ are given then the vertex M of the associated penumbra $P(M)$ is obtained by

$$M = m + \frac{r}{n} \frac{1}{\sqrt{1 - \frac{1}{n}}}\, E\,. \tag{3}$$

With this information at our disposal, we can reformulate the task of finding a suitable maximal matrix $\overline{A}$ dominating the matrices $\{A_1, \ldots, A_m\}$: The *smallest* sphere enclosing the spheres associated with $\{A_1, \ldots, A_m\}$ determines the matrix $\overline{A}$ that dominates the A_i. It is minimal in the sense, that there is no smaller one w.r.t. the Loewner ordering which has this "covering property" of its penumbra.
This is a non trivial problem of computational geometry and we tackle it by using a sophisticated algorithm implemented by B. Gaertner [20]. Given a set of points in $\mathbb{R}^d$ it is capable of finding the smallest ball enclosing these points. Hence for each $i = 1, \ldots, m$ we sample within the set of extreme points $\{A_i - \mathrm{trace}(A_i) v\, v^\top\}$ of the base of $P(A_i)$ by expressing v in 3d-spherical coordinates, $v = (\sin\phi\cos\psi, \sin\phi\sin\psi, \cos\phi)$ with $\phi \in [0, 2\pi[$, $\psi \in [0, \pi[$.
It is quite instructive to consider the case $n = 2$ which can be visualised by embedding $\mathrm{Sym}(2)$ in $\mathbb{R}^3$ via

$$A = (a_{ij})_{i,j=1,2} \longleftrightarrow \frac{1}{\sqrt{2}} \left(2a_{12}, a_{22} - a_{11}, a_{22} + a_{11}\right)^\top$$

as it is indicated in Figure 1(a). The transform is an isometry and maps $\{A \in \mathrm{Sym}(2) : \mathrm{trace}(A) = 0\}$ onto the x-y-plane. The extreme points are the matrices $vv^\top$ with $v^\top = (\cos\varphi, \sin\varphi)$ where $\varphi \in [0, 2\pi[$. Hence the aforementioned descriptive sets are discs in the x-y-plane determining the penumbras associated with the set of matrices. The penumbras of the matrices $\{A_1, \ldots, A_m\}$ are covered with the minimal penumbral cone whose vertex represents the desired maximal matrix $\overline{A}$. This minimal cone is found by calculating the smallest circle, its descriptive set, enclosing the discs stemming from the matrices $\{A_1, \ldots, A_m\}$.
The geometric point of view allows us to justify the usage of the Loewner ordering. To this end recall the formula

$$\max(a_1, a_2) \;=\; \frac{1}{2}(a_1 + a_2) + \frac{1}{2}|a_1 - a_2|\,. \tag{4}$$

valid for any real numbers a_1 and a_2. Let $\mathrm{diag}(\alpha_1, \ldots, \alpha_n)$ denote a diagonal matrix with entries $\alpha_1, \ldots, \alpha_n$. We define for a symmetric matrix $A \in \mathrm{Sym}(n)$ with eigenvalue decomposition $A = V\,\mathrm{diag}(\alpha_1, \ldots, \alpha_n)\,V^\top$ the matrix $|A|$ by

$$|A| := V\,\mathrm{diag}(|\alpha_1|, \ldots, |\alpha_n|)\,V^\top.$$

Then an elementary calculation in the case $n = 2$ (providing the smallest enclosing circle of two circles) reveals that the maximal matrix dominating A_1 and A_2 obtained through

$$\max(A_1, A_2) \;=\; \frac{1}{2}(A_1 + A_2) + \frac{1}{2}|A_1 - A_2|$$

indeed coincides with the maximal matrix induced by the Loewner ordering. This demonstrates that it is the Loewner ordering that stands behind the natural generalisation of this "algebraic maximum" in (4) to symmetric matrices. Note that an extension of this algebraic approach to sets of symmetric matrices with more than two elements is not feasible.
We summarise the above construction in four steps: In order to determine the maximal matrix $\overline{A}$ to a given set of matrices $\{A_1, \ldots, A_m\}$

1. calculate their projections a_i, $i = 1, \ldots, m$ according to (1),
2. determine the radii r_i, $i = 1, \ldots, m$, of the bases of their penumbras through (2),
3. determine the centre and radius of the smallest ball enclosing these bases,
4. recover the vertex of the associated penumbral cone via formula (3).

This definition is in fact *rotationally invariant*, that means, it satisfies

$$\max(VA_1V^\top, \ldots, VA_mV^\top) \;=\; V\,\max(A_1, \ldots, A_m)\,V^\top$$

for any orthogonal matrix V.
To see this we first recall that

$$\operatorname{trace}(VMV^\top) = \operatorname{trace}(M)$$

for any orthogonal matrix V. Hence the radii of the bases are unaltered by the V according to (2). In view of (1) the orthogonal projection m_i, the centres of the spheres, undergo the same transformation. Therefore their smallest enclosing ball evolves from the original one by the same rotational transformation. Finally, the vertex of the associated penumbral cone is just a rotated version of the original vertex as (3) indicates. Also *positive semidefiniteness is preserved* by construction:

$$\max(A_1, \ldots, A_m) \geq A_i \geq 0 \quad \text{for} \quad i = 1, \ldots, m\,.$$

Finally, the above maximum of symmetric matrices *depends continuously on the input matrices* since the associated projections and radii do so as the formulas (1) and (2) show. By its very definition the smallest enclosing ball, that is its centre and radius, as well as the associated penumbra with its vertex (3) depend continuously on its input points.

We do not rely on the relation $\min(a_1, a_2) \;=\; \frac{1}{2}\,(a_1 + a_2) \;-\; \frac{1}{2}\,|a_1 - a_2|$ with real numbers a_1, a_2 for the definition of an minimum, because it would lead to a notion which does not preserve positive semidefiniteness. Instead we take advantage of the relation

$$\min(A_1, \ldots, A_m) \;=\; \left(\max\left({A_1}^{-1}, \ldots, {A_m}^{-1}\right)\right)^{-1}$$

which is the matrix-valued counterpart of a readily established connection between maximum and minimum for positive real numbers $a_1, \ldots, a_m$.

The rotational invariance of this notion of an maximum carries over from the maximum since inversion of a matrix is a rotationally invariant operation:

$$(V^\top MV)^{-1} \;=\; V^{-1}M^{-1}(V^\top)^{-1} \;=\; V^\top M^{-1}V\,,$$

due to the orthogonality of the rotation matrix V.
Inversion also preserves the positiveness of matrices: If the eigenvalues λ_1,...,λ_n of a matrix M are positive, then so are the eigenvalues λ_1^{-1},...,λ_n^{-1} of M^{-1}.
At last, the continuity of the matrix inversion ensures the continuity of the minimum of matrices defined above.

4 Tensor-Valued Morphology

With these notions of minimum and maximum at our disposal the definitions of the morphological operations from Section 2 carry over essentially verbatim with one exception: The morphological Laplacian Δ_B as defined in Section 2 gives a matrix in the tensor-valued setting. We make use of the trace of the morphological Laplacian to steer the tensor-valued shock filter

$$S_B f_{i,j} := \begin{cases} f \oplus B & (\mathrm{trace}(\Delta_B f) < 0), \\ f & (\mathrm{trace}(\Delta_B f) = 0), \\ f \ominus B & (\mathrm{trace}(\Delta_B f) > 0), \end{cases}$$

where subscripts $i, j = 1, 2$ indicate the components of the corresponding matrices. It should be noted that unlike in the scalar-valued setting the minimum/maximum definitions are not associative in the tensor case. Thus a semi-group property of the derived dilation and erosion cannot be guaranteed. However, this has no effects as long as these morphological operations are not iterated. It is also worth noting that the matrix-valued morphological gradient approximates $\mathrm{Sup}_{\nu \in S^2}(\partial_\nu f)$ although it is no longer a particular directional derivative.

Positive definite matrices $A \in \mathbb{R}^{3\times 3}$ can be visualised as ellipsoids

$$\left\{ x \in \mathbb{R}^3 : x^\top A^{-2} x = 1 \right\},$$

that is as a level set of the quadratic form $x^\top A^{-2} x$. In this geometric context the minimum is represented by an ellipse that is contained in each of the ellipses of the given set of matrices. The ellipse representing the maximum surrounds all ellipse of the matrix set.
There is a natural interpretation of this ellipsoid in the context of diffusion tensors: Assuming that a particle is initially located in the origin and is subject to the diffusivity A, then the ellipsoid encloses the smallest volume within which this particle will be found with some required probability after a short time interval. The minimum and maximum of two positive definite 2×2 matrices are displayed in Figure 1.

5 Experimental Results

For our numerical experiments we use a $128 \times 128 \times 30$ field of 3-D tensors originating from a positive definite 3-D DT-MRI data set of a human head. For detailed information about the acquisition of this data type the reader

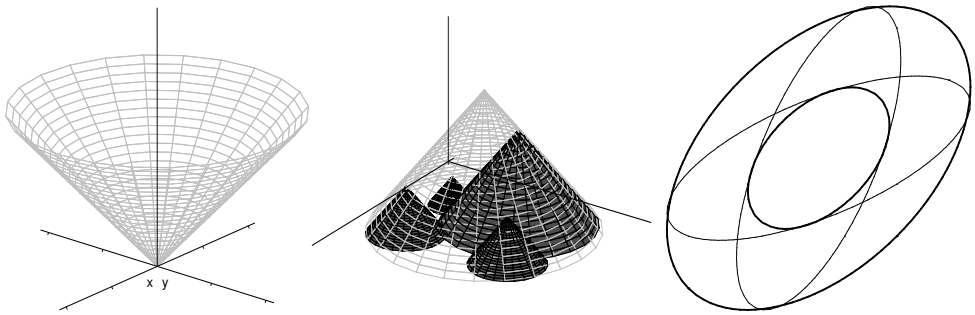

Figure 1: **(a) Left:** The cone corresponding to the Loewner cone depicted in $\mathbb{R}^3$. **(b) Middle:** Penumbras of various matrices together with the smallest covering penumbra. The tip of this penumbra marks the maximum of the matrices under consideration. **(c) Right:** The maximum (largest ellipse) and minimum (smallest ellipse) of two 2×2-matrices.

is referred to [5] and the literature cited there.
Figure 2 (a) exhibits a 128×128 layer of these data while (b) displays an enlarged section near the upper right corner of (a). We will visualise the effect of the various morphological operations mentioned above by having a closer look at this very section.
The data are represented as ellipsoids via the level sets of the quadratic form $\{x^\top A^{-2} x : x \in \mathbb{R}^3\}$ associated with a matrix $A \in \mathrm{Sym}^+(3)$. In using A^{-2} the length of the semi-axes of the ellipsoid correspond directly with the three eigenvalues of the positive definite matrix. A technical issue is that our data set contains not only positive definite matrices. Because of the quantisation there are singular matrices (particularly, a lot of zero matrices outside the head segment) and even matrices with negative eigenvalues. The negative values are of very small absolute value, and they result from measurement imprecision and quantisation errors. While such values do not pose a problem in the dilation process, the erosion, relying on inverses of positive definite matrices, has to be regularised. Instead of the exact inverse A^{-1} of a given matrix A we use $(A + \varepsilon I)^{-1}$
Figure 3 shows dilations while Figure 4 displays erosions with three different structuring elements, a stencil approximating a disk of radius 2, indicated by BSE(2), a rod-shaped stencil in y-direction of length 3 and "thickness"

1, and a similar stencil in z-direction, denoted by y-RSE(3) and z-RSE(3), respectively. The z-direction is perpendicular to the image plane. Hence the morphological operations utilizing z-RSE(3) and BSE(2) involve layers not displayed here.
As known from scalar-valued morphology, the shape of details in the dilated and eroded images mirrors the shape of the structuring element. In agreement with the scalar valued case we observe dilation to result in an extension of areas with matrices having relatively large eigenvalues, that is, large semi-achses of the representing ellipsoids. Clearly this extension is more prominent for the structuring element BSE(2) in comparison with y-RSE(3) and z-RSE(3).
We will observe this effect in general: the impact of a morphological operation is more pronounced when BSE(2) is used than in the case of y-RSE(3) and z-RSE(3) since the first structuring element contains more voxels.
As expected mid-range filtering results in blurring of the original image, see Figures 5. Generally speaking, the larger the structuring element, the more pronounced the blurring effect.
Figures 6 and 7 display the results of opening and closing operations with the three structuring elements. In good analogy to their scalar-valued counterparts, both operations restitute the coarse shape and size of structures while eliminating small-scale details formed by small (closing) or large (erosion) values, respectively.
The top hat filters can be seen in Figures 8, 9, and 10. As in the scalar-valued case, the white top hat (Figure 8) is sensitive for small-scale details formed by values of high magnitude, i.e. matrices with generally large eigenvalues. At locations where such details are present, the matrices in the white top-hat image are quite large. The black top hat (figure 9) exhibits contrary behaviour, responding with high values to small-scale details involving matrices with relatively high anisotropy.
That they correspond indeed to two complementary classes of details becomes clear from the third top-hat filter, the self-dual top-hat. It is the sum of the white and black top hats which is also apparent from Figure 10. Note that each of the three top hats eliminates the matrices in the prominent and homegenous area in the northern central part of the original image 2(b). This relatively large area violates the condition of being a "small-scale detail", hence the top hats output matrices that are too small to be displayed.
Figures 13, 12, and 11 show morphological derivative operators. Just as their scalar analogs, internal and external morphological gradients behave similar, both reveal a sensitivity for edge-like structures. The Beucher gradient is the sum of the external and internal gradient. This washes out the information provided by the "one-sided" gradients. A similar effect is observed in scalar

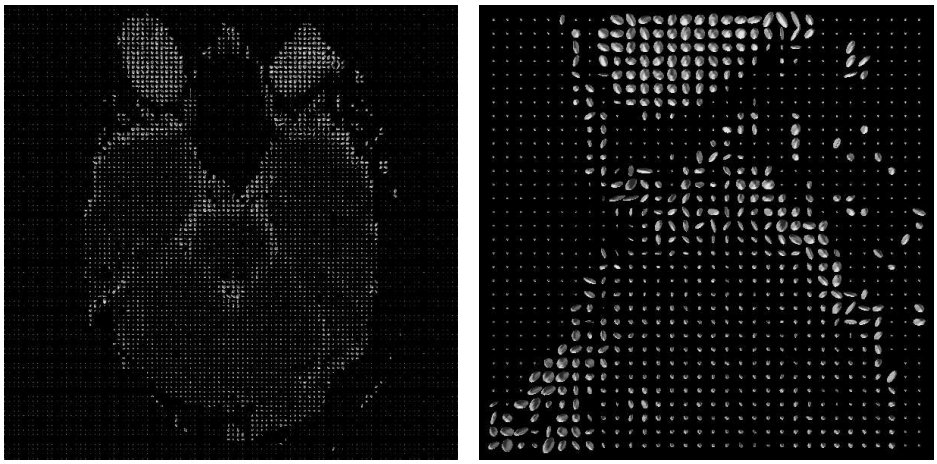

Figure 2: **(a) Left:** A slice of a 3-D tensor field extracted from a DT-MRI data set of a human head. **(b) Right:** Enlargement of a section in the upper right corner of (a).

morphology.
The Laplacian Δ_{m} which is computed as the difference of the external and internal gradient, produces positive definite matrices as well as indefinite and negative definite ones. This is the explanation for the void areas in the images 14: non-positive definite matrices cannot be displayed as ellipsoids and hence are omitted. Figure 15 demonstrates how the Laplacian can be used to control a shock filter. While applying dilation in pixels where the trace of the Laplacian is negative, it uses erosion wherever the trace of the Laplacian is positive. The result is an amplification of the structures present in the original image 2(b) leading to a segmentation-like output.
All the examples of morphological operators feature strong dependence on the type and shape of the employed structuring element. This is typical for morphology both in the scalar- and in the matrix-valued case. And it is this feature that constitutes the versatility of morphological techniques.

6 Conclusions

In this paper we have extended fundamental concepts of mathematical morphology to the case of 3-dimensional matrix-valued data. Based on the Loewner ordering for symmetric matrices novel notions of maximum and minimum of a set of symmetric 3×3-matrices have been proposed. These

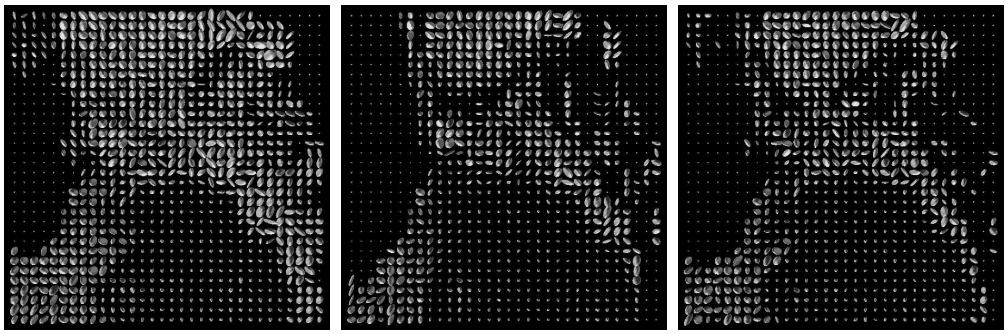

Figure 3: **(a) Left:** Dilation with BSE(2) stencil. **(a) Middle:** Same with y-RSE(3) stencil. **(b) Right:** Same with z-RSE(3) stencil.

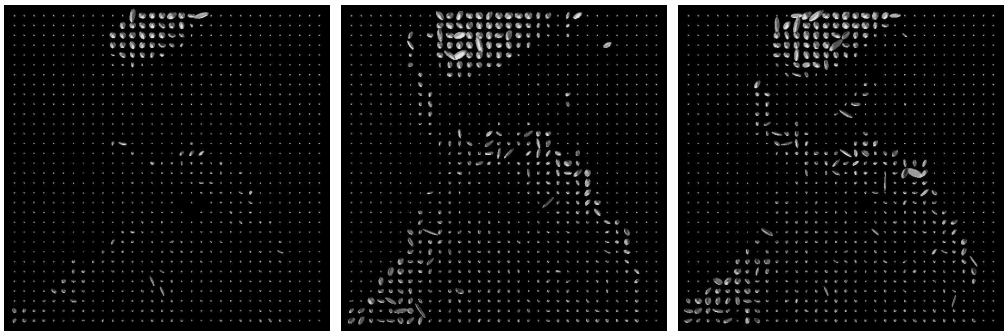

Figure 4: **(a) Left:** Erosion with BSE(2) stencil. **(a) Middle:** Same with y-RSE(3) stencil. **(b) Right:** Same with z-RSE(3) stencil.

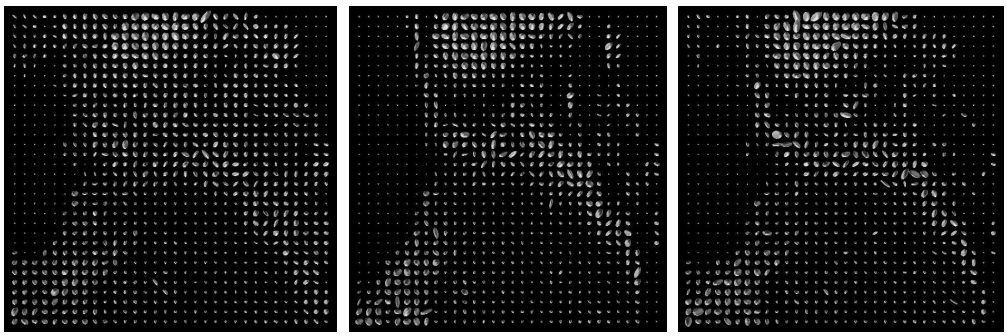

Figure 5: **(a) Left:** Mid-range filter with BSE(2) stencil. **(a) Middle:** same with y-RSE(3) stencil. **(b) Right:** same with z-RSE(3) stencil.

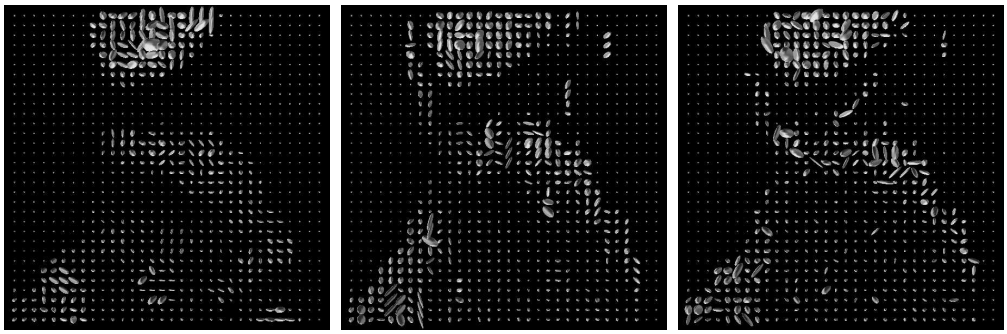

Figure 6: **(a) Left:** Opening with BSE(2) stencil. **(a) Middle:** Same with y-RSE(3) stencil. **(b) Right:** Same with z-RSE(3) stencil.

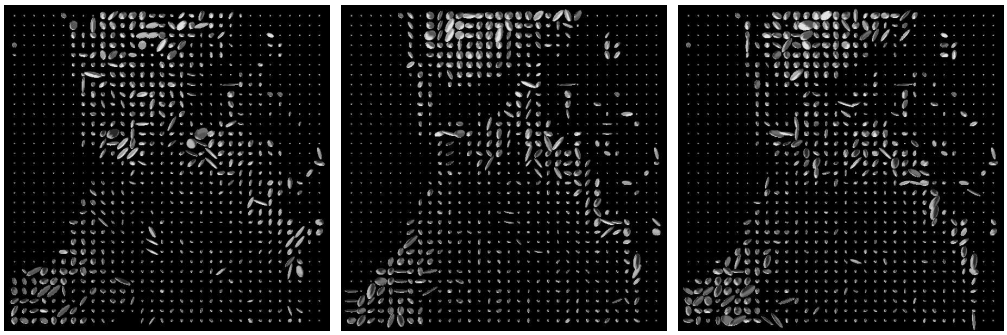

Figure 7: **(a) Left:** Closing with BSE(2) stencil. **(a) Middle:** Same with y-RSE(3) stencil. **(b) Right:** Same with z-RSE(3) stencil.

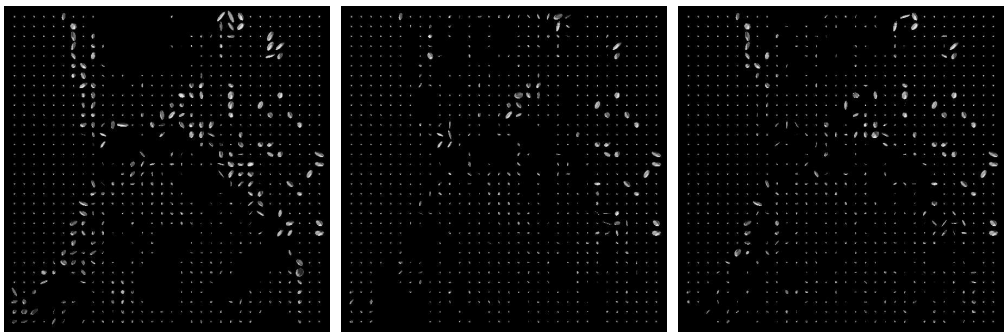

Figure 8: **(a) Left:** White top hat with BSE(2) stencil. **(a) Middle:** Same with y-RSE(3) stencil. **(b) Right:** Same with z-RSE(3) stencil.

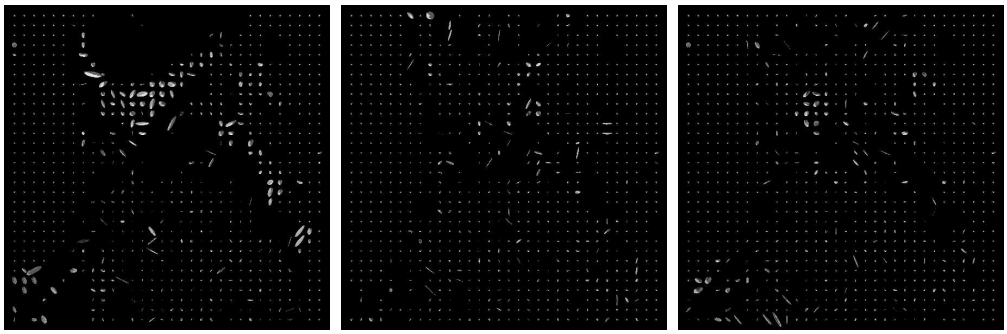

Figure 9: **(a) Left:** Black top hat with BSE(2) stencil. **(a) Middle:** Same with y-RSE(3) stencil. **(b) Right:** Same with z-RSE(3) stencil.

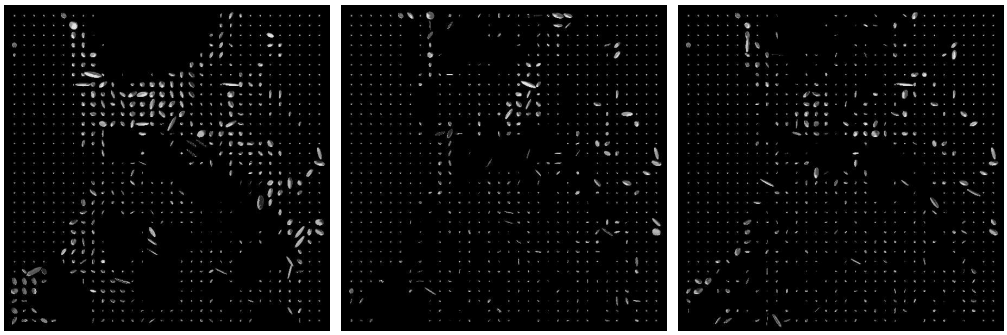

Figure 10: **(a) Left:** Self-dual top hat with BSE(2) stencil. **(a) Middle:** Same with y-RSE(3) stencil. **(b) Right:** Same with z-RSE(3) stencil.

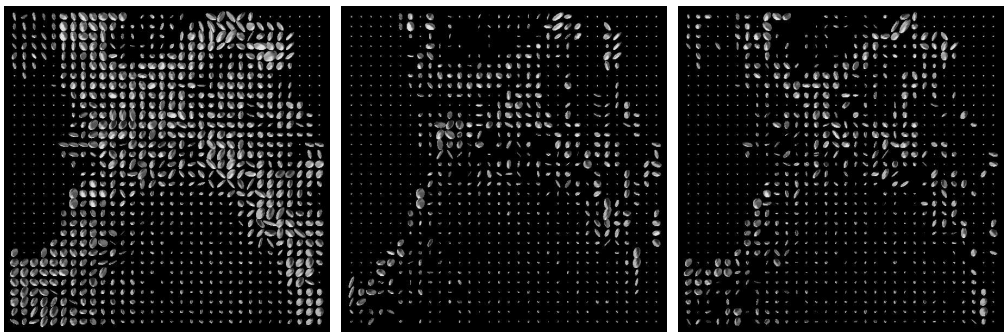

Figure 11: **(a) Left:** Beucher-gradient with BSE(2) stencil. **(a) Middle:** Same with y-RSE(3) stencil. **(b) Right:** Same with z-RSE(3) stencil.

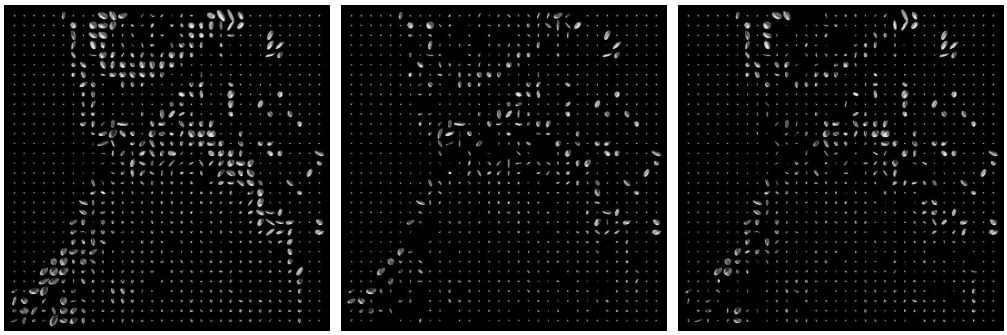

Figure 12: **(a) Left:** Internal-gradient with BSE(2) stencil. **(a) Middle:** Same with y-RSE(3) stencil. **(b) Right:** Same with z-RSE(3) stencil.

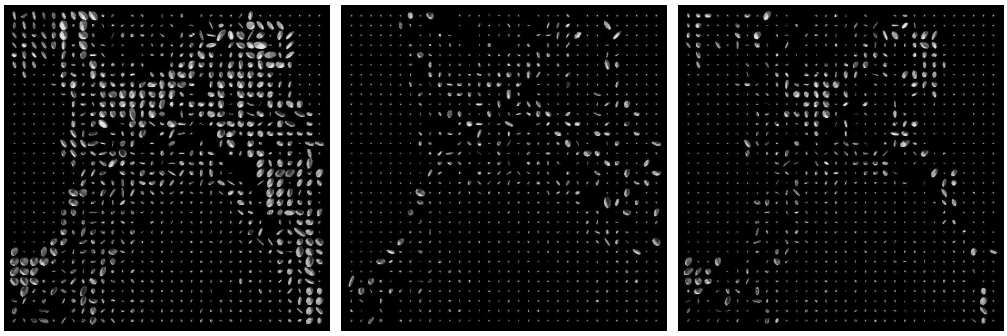

Figure 13: **(a) Left:** External-gradient with BSE(2) stencil. **(a) Middle:** Same with y-RSE(3) stencil. **(b) Right:** Same with z-RSE(3) stencil.

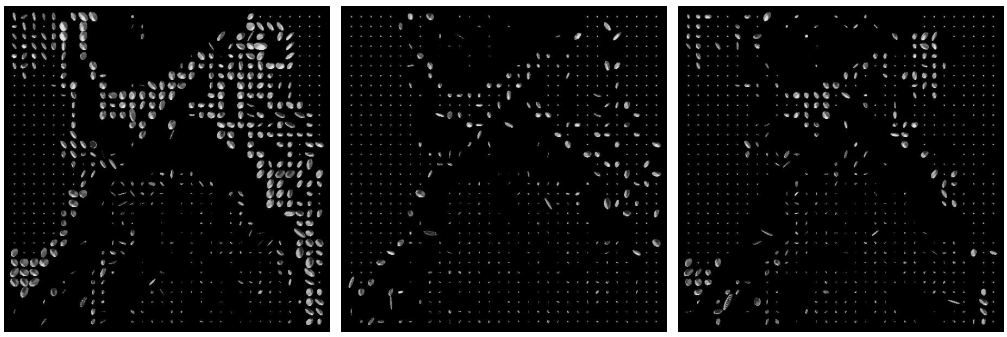

Figure 14: **(a) Left:** Morphological Laplacian with BSE(2) stencil. **(a) Middle:** Same with y-RSE(3) stencil. **(b) Right:** Same with z-RSE(3) stencil.

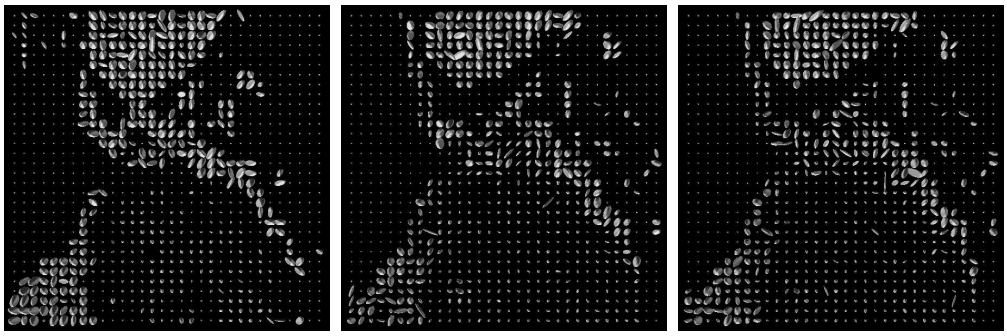

Figure 15: **(a) Left:** Shock filtering with BSE(2) stencil. **(a) Middle:** Same with y-RSE(3) stencil. **(b) Right:** Same with z-RSE(3) stencil.

notions extend the corresponding scalar-valued concept. They exhibit invariance, positivity, and continuity properties essential for their use in the design of morphological operations for matrix-valued data. For this reason we have succeeded to generalise not only standard morphological operations but also morphological derivatives and shock filters to the matrix-valued setting. The technique developed for this purpose is considerably more general and sustainable than former approaches for the case of 2×2-matrices introduced in [12]. The extended approach holds the potential to cope with 4×4-matrices or larger.

In the experimental part we have contrasted three types of structuring elements with respect to their effect on actual 3D-DT-MRI data. Very satisfyingly they feature the same characteristics as their scalar-valued counterparts. In future investigations we will explore the filtering capabilities of various operators within the wide framework of morphology. In doing so we will apply morphological operators not only to positive definite matrix fields but also to indefinite/negative definite matrix data sets.

Acknowledgements

We are grateful to Anna Vilanova i Bartrolí (Biomedical Imaging Group, TU Eindhoven) and Carola van Pul (Maxima Medical Center, Eindhoven) for providing us with the DT-MRI data set. We also would like to thank Stephan Zimmer for his support concerning visualisation issues.

References

[1] L. Alvarez and L. Mazorra. Signal and image restoration using shock filters and anisotropic diffusion. *SIAM Journal on Numerical Analysis*, 31:590–605, 1994.

[2] J. Astola, P. Haavisto, and Y. Neuvo. Vector median filters. *Proceedings of the IEEE*, 78(4):678–689, 1990.

[3] V. Barnett. The ordering of multivariate data. *Journal of the Royal Statistical Society A*, 139(3):318–355, 1976.

[4] A. Barvinok. *A Course in Convexity*, volume 54 of *Graduate Studies in Mathematics*. American Mathematical Society, Providence, 2002.

[5] P. J. Basser. Inferring microstructural features and the physical state of tissues from diffusion-weighted images. *Nuclear Magnetic Resonance in Biomedicine*, 8:333–334, 1995.

[6] P. J. Basser, J. Mattiello, and D. LeBihan. MR diffusion tensor spectroscopy and imaging. *Biophysical Journal*, 66:259–267, 1994.

[7] S. Beucher and C. Lantuéjoul. Use of watersheds in contour detection. In *Proc. International Workshop on Image Processing, Real-Time Edge and Motion Detection/Estimation*, pages 2.1–2.12, Rennes, France, September 1979. IRISA Report No. 131.

[8] J. Bigün, G. H. Granlund, and J. Wiklund. Multidimensional orientation estimation with applications to texture analysis and optical flow. *IEEE Transactions on Pattern Analysis and Machine Intelligence*, 13(8):775–790, August 1991.

[9] J. M. Borwein and A. S. Lewis. *Convex Analysis and Nonlinear Optimization*. Springer, New York, 1999.

[10] T. Brox, M. Rousson, R. Deriche, and J. Weickert. Unsupervised segmentation incorporating colour, texture, and motion. In N. Petkov and M. A. Westenberg, editors, *Computer Analysis of Images and Patterns*, volume 2756 of *Lecture Notes in Computer Science*, pages 353–360. Springer, Berlin, 2003.

[11] T. Brox and J. Weickert. Nonlinear matrix diffusion for optic flow estimation. In L. Van Gool, editor, *Pattern Recognition*, volume 2449 of *Lecture Notes in Computer Science*, pages 446–453. Springer, Berlin, 2002.

[12] B. Burgeth, M. Welk, C. Feddern, and J. Weickert. Morphological operations on matrix-valued images. In T. Pajdla and J. Matas, editors, *Computer Vision – ECCV 2004*, volume 3024 of *Lecture Notes in Computer Science*, pages 155–167. Springer, Berlin, 2004.

[13] B. Burgeth, M. Welk, C. Feddern, and J. Weickert. Mathematical morphology on tensor data using the loewner ordering. In H. Hagen J. Weickert, editor, *Visualization and Processing of Tensor Fields*. Springer, Berlin, 2005. to appear.

[14] V. Caselles, G. Sapiro, and D. H. Chung. Vector median filters, inf-sup convolutions, and coupled PDE's: theoretical connections. *Journal of Mathematical Imaging and Vision*, 12(2):109–119, April 2000.

[15] C. A. Castaño Moraga, C.-F. Westin, and J. Ruiz-Alzola. Homomorphic filtering of DT-MRI fields. In R. E. Ellis and T. M. Peters, editors, *Medical Image Computing and Computer-Assisted Intervention – MICCAI 2003*, Lecture Notes in Computer Science. Springer, Berlin, 2003.

[16] M. L. Comer and E. J. Delp. Morphological operations for color image processing. *Journal of Electronic Imaging*, 8(3):279–289, 1999.

[17] O. Coulon, D. C. Alexander, and S. A. Arridge. A regularization scheme for diffusion tensor magnetic resonance images. In M. F. Insana and R. M. Leahy, editors, *Information Processing in Medical Imaging – IPMI 2001*, volume 2082 of *Lecture Notes in Computer Science*, pages 92–105. Springer, Berlin, 2001.

[18] C. Feddern, J. Weickert, and B. Burgeth. Level-set methods for tensor-valued images. In O. Faugeras and N. Paragios, editors, *Proc. Second IEEE Workshop on Geometric and Level Set Methods in Computer Vision*, pages 65–72, Nice, France, October 2003. INRIA.

[19] W. Förstner and E. Gülch. A fast operator for detection and precise location of distinct points, corners and centres of circular features. In *Proc. ISPRS Intercommission Conference on Fast Processing of Photogrammetric Data*, pages 281–305, Interlaken, Switzerland, June 1987.

[20] B. Gärtner. http://www.inf.ethz.ch/personal/gaertner/. WebPage last visited: December 2nd, 2005.

[21] G. Gilboa, N. A. Sochen, and Y. Y. Zeevi. Regularized shock filters and complex diffusion. In A. Heyden, G. Sparr, M. Nielsen, and P. Johansen,

editors, *Computer Vision – ECCV 2002*, volume 2350 of *Lecture Notes in Computer Science*, pages 399–413. Springer, Berlin, 2002.

[22] J. Goutsias, H. J. A. M. Heijmans, and K. Sivakumar. Morphological operators for image sequences. *Computer Vision and Image Understanding*, 62:326–346, 1995.

[23] J. Goutsias, L. Vincent, and D. S. Bloomberg, editors. *Mathematical Morphology and its Applications to Image and Signal Processing*, volume 18 of *Computational Imaging and Vision*. Kluwer, Dordrecht, 2000.

[24] G. H. Granlund and H. Knutsson. *Signal Processing for Computer Vision*. Kluwer, Dordrecht, 1995.

[25] F. Guichard and J.-M. Morel. Partial differential equations and image iterative filtering. In I. S. Duff and G. A. Watson, editors, *The State of the Art in Numerical Analysis*, number 63 in IMA Conference Series (New Series), pages 525–562. Clarendon Press, Oxford, 1997.

[26] F. Guichard and J.-M. Morel. A note on two classical enhancement filters and their associated PDE's. *International Journal of Computer Vision*, 52(2/3):153–160, 2003.

[27] K. Hahn, S. Pigarin, and B. Pütz. Edge preserving regularization and tracking for diffusion tensor imaging. In W. J. Niessen and M. A. Viergever, editors, *Medical Image Computing and Computer-Assisted Intervention – MICCAI 2001*, volume 2208 of *Lecture Notes in Computer Science*, pages 195–203. Springer, Berlin, 2001.

[28] R. M. Haralick. Digital step edges from zero crossing of second directional derivatives. *IEEE Transactions on Pattern Analysis and Machine Intelligence*, 6(1):58–68, 1984.

[29] R. M. Haralick, S. R. Sternberg, and X. Zhuang. Image analysis using mathematical morphology. *IEEE Transactions on Pattern Analysis and Machine Intelligence*, 9(4):532–550, July 1987.

[30] R. Hardie and G. Arce. "Ranking in R^p" and its use in multivariate image estimation. *IEEE Transactions on Circuits, Systems and Video Technology*, 1(2):197–209, 1991.

[31] C. G. Harris and M. Stephens. A combined corner and edge detector. In *Proc. Fouth Alvey Vision Conference*, pages 147–152, Manchester, England, August 1988.

[32] H. J. A. M. Heijmans. *Morphological Image Operators*. Academic Press, Boston, 1994.

[33] H. J. A. M. Heijmans and J. B. T. M. Roerdink, editors. *Mathematical Morphology and its Applications to Image and Signal Processing*, volume 12 of *Computational Imaging and Vision*. Kluwer, Dordrecht, 1998.

[34] J.-B. Hiriart-Urruty and C. Lemarechal. *Fundamentals of Convex Analysis*. Springer, Heidelberg, 2001.

[35] R. Kimmel and A. M. Bruckstein. Regularized Laplacian zero crossings as optimal edge integrators. *International Journal of Computer Vision*, 53(3):225–243, 2003.

[36] H. P. Kramer and J. B. Bruckner. Iterations of a non-linear transformation for enhancement of digital images. *Pattern Recognition*, 7:53–58, 1975.

[37] G. Louverdis, M. I. Vardavoulia, I. Andreadis, and P. Tsalides. A new approach to morphological color image processing. *Pattern Recognition*, 35:1733–1741, 2002.

[38] D. Marr and E. Hildreth. Theory of edge detection. *Proceedings of the Royal Society of London, Series B*, 207:187–217, 1980.

[39] G. Matheron. *Eléments pour une théorie des milieux poreux*. Masson, Paris, 1967.

[40] G. Matheron. *Random Sets and Integral Geometry*. Wiley, New York, 1975.

[41] G. Medioni, M.-S. Lee, and C.-K. Tang. *A Computational Framework for Segmentation and Grouping*. Elsevier, Amsterdam, 2000.

[42] S. Osher and L. Rudin. Shocks and other nonlinear filtering applied to image processing. In A. G. Tescher, editor, *Applications of Digital Image Processing XIV*, volume 1567 of *Proceedings of SPIE*, pages 414–431. SPIE Press, Bellingham, 1991.

[43] S. Osher and L. I. Rudin. Feature-oriented image enhancement using shock filters. *SIAM Journal on Numerical Analysis*, 27:919–940, 1990.

[44] G. J. M. Parker, J. A. Schnabel, M. R. Symms, D. J. Werring, and G. J. Barker. Nonlinear smoothing for reduction of systematic and random errors in diffusion tensor imaging. *Journal of Magnetic Resonance Imaging*, 11:702–710, 2000.

[45] C. Pierpaoli, P. Jezzard, P. J. Basser, A. Barnett, and G. Di Chiro. Diffusion tensor MR imaging of the human brain. *Radiology*, 201(3):637–648, December 1996.

[46] C. Poupon, J.-F. Mangin, V. Frouin, J. Régis, F. Poupon, M. Pachot-Clouard, D. Le Bihan, and I. Bloch. Regularization of MR diffusion tensor maps for tracking brain white matter bundles. In W. M. Wells, A. Colchester, and S. Delp, editors, *Medical Image Computing and Computer-Assisted Intervention – MICCAI 1998*, volume 1496 of *Lecture Notes in Computer Science*, pages 489–498. Springer, Berlin, 1998.

[47] A. R. Rao and B. G. Schunck. Computing oriented texture fields. *CVGIP: Graphical Models and Image Processing*, 53:157–185, 1991.

[48] L. Remaki and M. Cheriet. Numerical schemes of shock filter models for image enhancement and restoration. *Journal of Mathematical Imaging and Vision*, 18(2):153–160, March 2003.

[49] M. Rousson, T. Brox, and R. Deriche. Active unsupervised texture segmentation on a diffusion based feature space. In *Proc. 2003 IEEE Computer Society Conference on Computer Vision and Pattern Recognition*, volume 2, pages 699–704, Madison, WI, June 2003. IEEE Computer Society Press.

[50] J. G. M. Schavemaker, M. J. T. Reinders, and R. van den Boomgaard. Image sharpening by morphological filtering. In *Proc. 1997 IEEE Workshop on Nonlinear Signal and Image Processing*, Mackinac Island, MI, September 1997. www.ecn.purdue.edu/NSIP/.

[51] J. Serra. *Echantillonnage et estimation des phénomènes de transition minier*. PhD thesis, University of Nancy, France, 1967.

[52] J. Serra. *Image Analysis and Mathematical Morphology*, volume 1. Academic Press, London, 1982.

[53] J. Serra. *Image Analysis and Mathematical Morphology*, volume 2. Academic Press, London, 1988.

[54] P. Soille. *Morphological Image Analysis*. Springer, Berlin, 1999.

[55] S. R. Sternberg. Grayscale morphology. *Computer Vision, Graphics and Image Processing*, 35:333–355, 1986.

[56] H. Talbot and R. Beare, editors. *Proc. Sixth International Symposium on Mathematical Morphology and its Applications*. Sydney, Australia, April 2002. http://www.cmis.csiro.au/ismm2002/proceedings/.

[57] H. Talbot, C. Evans, and R. Jones. Complete ordering and multivariate mathematical morphology. In H. J. A. M. Heijmans and J. B. T. M. Roerdink, editors, *Mathematical Morphology and its Applications to Image and Signal Processing*, volume 12 of *Computational Imaging and Vision*. Kluwer, Dordrecht, 1998.

[58] D. Tschumperlé and R. Deriche. Diffusion tensor regularization with contraints preservation. In *Proc. 2001 IEEE Computer Society Conference on Computer Vision and Pattern Recognition*, volume 1, pages 948–953, Kauai, HI, December 2001. IEEE Computer Society Press.

[59] L. J. van Vliet, I. T. Young, and A. L. D. Beckers. A nonlinear Laplace operator as edge detector in noisy images. *Computer Vision, Graphics and Image Processing*, 45(2):167–195, 1989.

[60] J. Weickert. Coherence-enhancing shock filters. In B. Michaelis and G. Krell, editors, *Pattern Recognition*, volume 2781 of *Lecture Notes in Computer Science*, pages 1–8, Berlin, 2003. Springer.

[61] J. Weickert and T. Brox. Diffusion and regularization of vector- and matrix-valued images. In M. Z. Nashed and O. Scherzer, editors, *Inverse Problems, Image Analysis, and Medical Imaging*, volume 313 of *Contemporary Mathematics*, pages 251–268. AMS, Providence, 2002.

[62] M. Welk, C. Feddern, B. Burgeth, and J. Weickert. Median filtering of tensor-valued images. In B. Michaelis and G. Krell, editors, *Pattern Recognition*, volume 2781 of *Lecture Notes in Computer Science*, pages 17–24, Berlin, 2003. Springer.

[63] C.-F. Westin, S. E. Maier, B. Khidhir, P. Everett, F. A. Jolesz, and R. Kikinis. Image processing for diffusion tensor magnetic resonance imaging. In C. Taylor and A. Colchester, editors, *Medical Image Computing and Computer-Assisted Intervention – MICCAI 1999*, volume 1679 of *Lecture Notes in Computer Science*, pages 441–452. Springer, Berlin, 1999.